Journal of Alloys and Compounds 509 (2011) 922–928

Contents lists available at ScienceDirect

Journal of Alloys and Compounds

journal homepage: www.elsevier.com/locate/jallcom

Effect of grain shape on the texture evolution during cold rolling of Al–Mg alloys

H. Yuan[a], Q.F. Wang[a], J.W. Zhang[a], W.C. Liu[a,*], Y.K. Gao[b]

[a] Key Laboratory of Metastable Materials Science and Technology, College of Materials Science and Engineering, Yanshan University, No. 438 Hebei Avenue, Qinhuangdao, Hebei 066004, China

[b] Beijing Institute of Aeronautical Materials, Beijing 100095, China

ARTICLE INFO

Article history:
Received 8 July 2010
Received in revised form
19 September 2010
Accepted 22 September 2010
Available online 29 September 2010

Keywords:
Aluminum
Cold rolling
Texture
X-ray diffraction
Grain shape

ABSTRACT

The hot bands of continuous cast AA 5754 and high-Fe AA 5754 aluminum alloys exhibited elongated grains in the rolling direction after recrystallization annealing. The annealed hot bands were cold rolled to different reductions along the original rolling direction and transverse direction, respectively. The effect of grain shape on texture evolution was investigated by X-ray diffraction. It was found that straight-rolling resulted in a higher rate of disappearance of the r-cube + cube component and a slightly higher rate of formation of the β fiber component than cross-rolling. The elongated grains in the rolling direction were easier to rotate from initial orientations to the β fiber in straight-rolling than in cross-rolling.

1. Introduction

The texture evolution of aluminum alloys during rolling and subsequent annealing has long been a subject of research as the anisotropy of mechanical properties is significantly influenced by the texture developed during processing [1–5]. During rolling initial orientations are gradually rotated into the stable end orientations located on the β fiber, which runs from the brass (B) orientation {1 1 0} ⟨1 1 2⟩ through the S orientation {1 2 3} ⟨6 3 4⟩ to the copper (C) orientation {1 1 2} ⟨1 1 1⟩ [1,2]. Texture evolution during rolling is strongly affected by alloy composition, initial microstructure and texture prior to cold rolling. It is widely established that the initial texture has a large impact on rolling texture evolution [6–9]. The formation rate of the β fiber decreases as the initial texture changes from the r-cube texture to the cube texture [8]. The strong impact of the initial texture on rolling texture may overshadow the influence of other material parameters. It has been shown that a decrease in initial grain size leads to an accelerated rate of rolling texture evolution [10,11]. Deformation temperature also affects the texture evolution during rolling of aluminum alloys [12,13].

Quantification of texture evolution during rolling and subsequent annealing is very important for the prediction and control of texture in aluminum alloy sheets. Much research effort has been devoted to the modeling of rolling and recrystallization textures, with either empirically or mathematically based and physically based models [14–25]. Deformation texture is often simulated by using the full or relaxed constraints version of the Taylor–Bishop–Hill model [14–16], a rate-sensitive crystal plasticity model [17,18], and finite element calculations [19]. However, these models do not allow the precise texture prediction since they cannot account for the effect of alloy composition and initial microstructure on the rolling texture. Many efforts to develop more complex polycrystal plasticity models have been undertaken [20–22]. On the other hand, the texture evolution can be evaluated by the variation in texture volume fractions with rolling true strain. In order to quantify the texture evolution of AA 5000 series aluminum alloys, Liu and Morris [26,27] have improved the integration method of calculating texture volume fractions and established empirical formulae of texture volume fractions and rolling true strain by using equations of the Johnson–Mehl–Avrami–Kolmogorov (JMAK) type. The simple relations have been used to quantify the texture evolution during rolling of aluminum alloys [28–31].

The effect of grain shape on the yield strength anisotropy [32] and earing behavior [33] of Al–Li alloy sheet as well as the planar anisotropy of rolled steel sheets [34] has been reported. However, the effect of grain shape on rolling texture evolution remains unclear. In the present work, AA 5754 and high-Fe AA 5754 aluminum alloys with elongated grains were cold rolled to different reductions along the original rolling direction (RD) and transverse direction (TD), respectively. The effect of grain shape on texture evolution was analyzed quantitatively.

* Corresponding author. Tel.: +86 335 8074795; fax: +86 335 8074545.
E-mail address: wcliu@ysu.edu.cn (W.C. Liu).

0925-8388/$ – see front matter © 2010 Elsevier B.V. All rights reserved.
doi:10.1016/j.jallcom.2010.09.131

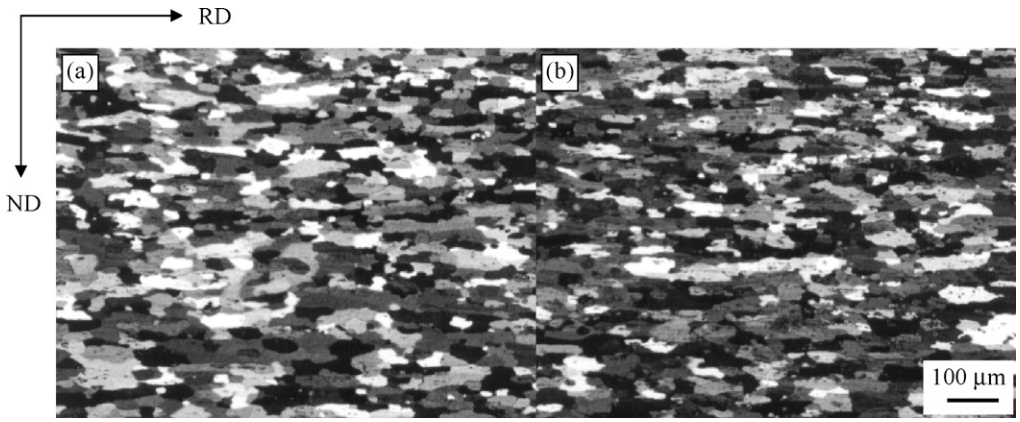

Fig. 1. Microstructure of the annealed hot bands of (a) AA 5754 and (b) high-Fe AA 5754 aluminum alloys.

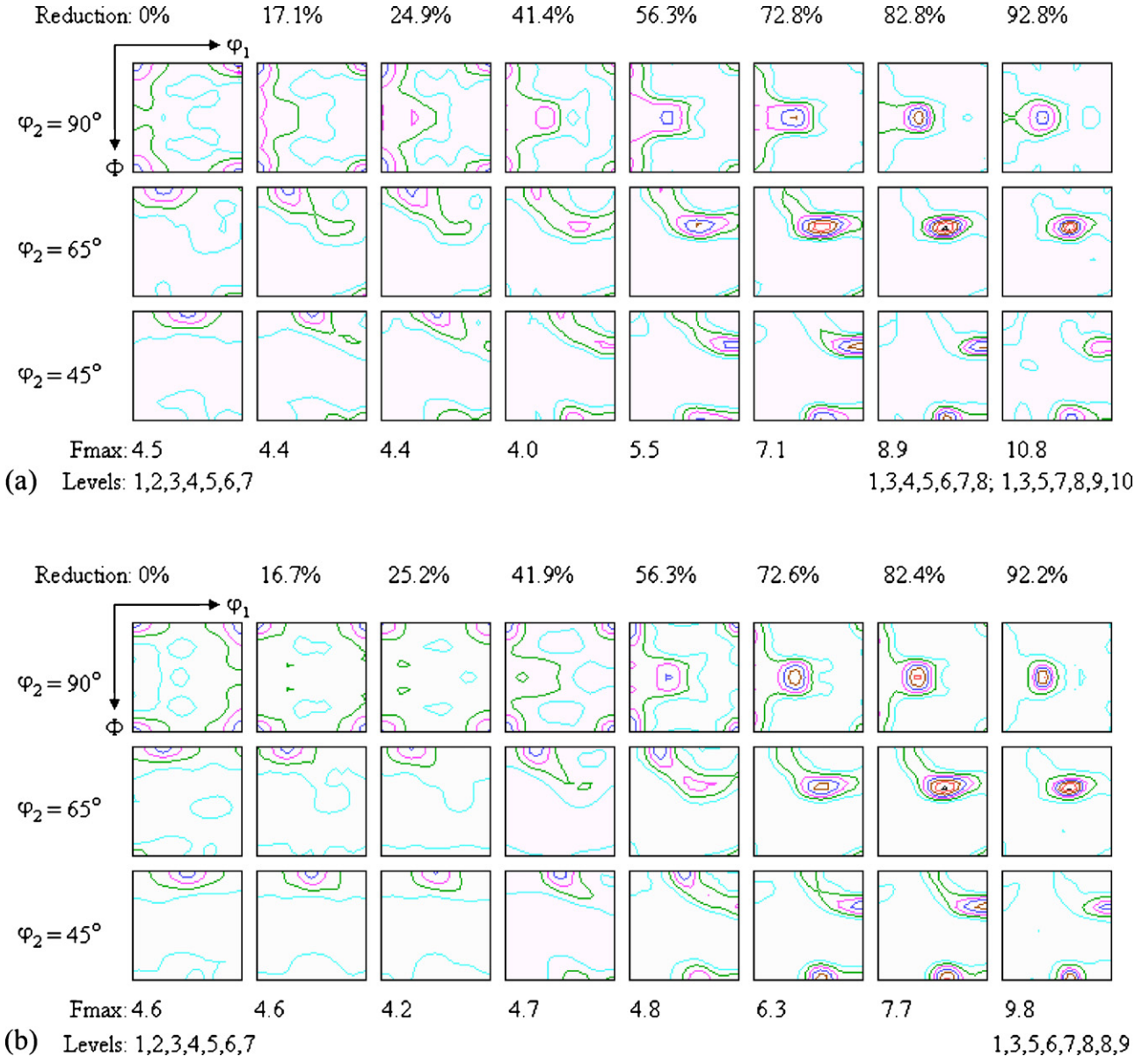

Fig. 2. Texture evolution of AA 5754 aluminum alloy during rolling along the original (a) RD and (b) TD.

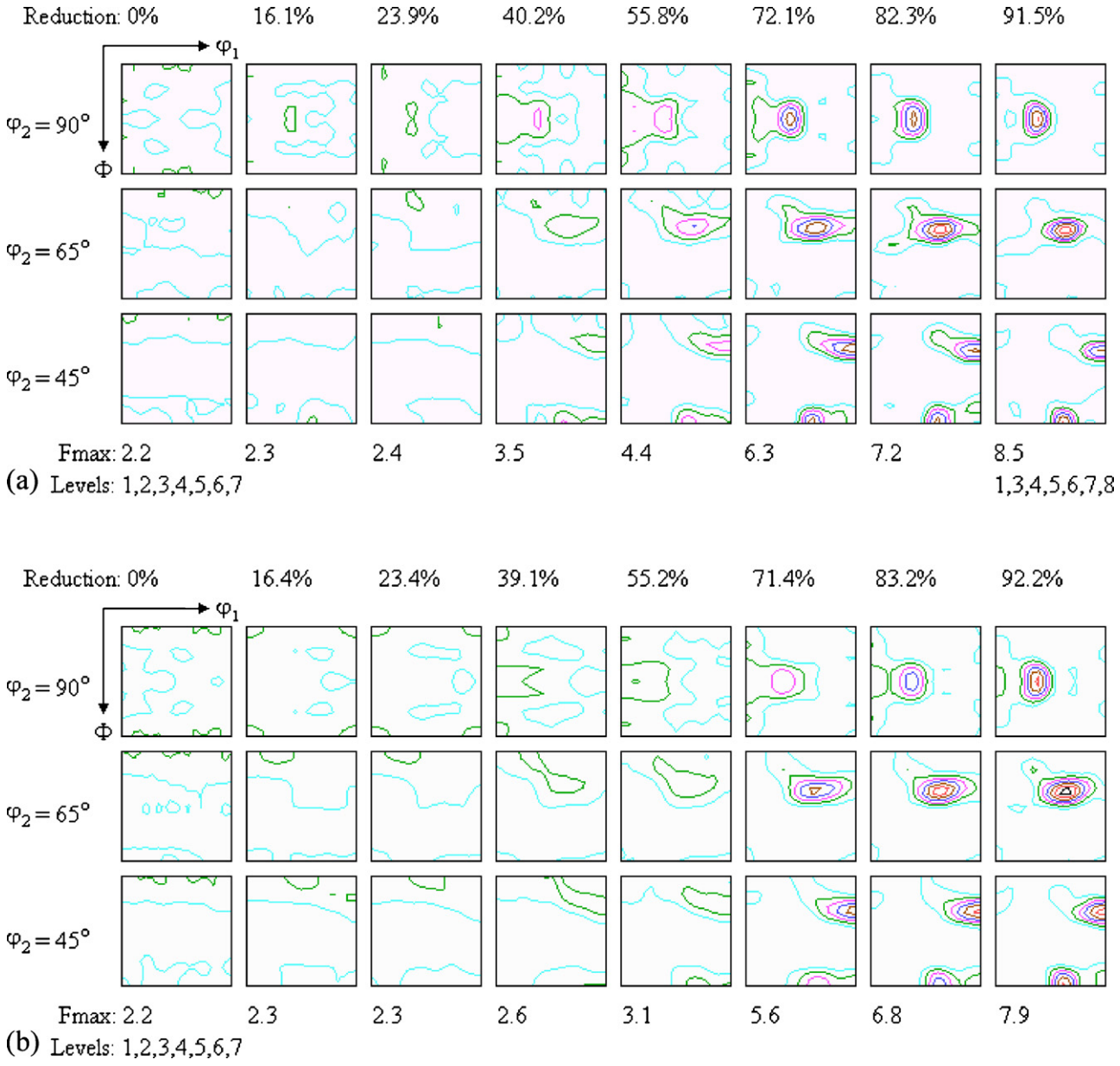

Fig. 3. Texture evolution of high-Fe AA 5754 aluminum alloy during rolling along the original (a) RD and (b) TD.

2. Experimental

The materials used in the present investigation were AA 5754 and high-Fe AA 5754 aluminum alloys. The chemical compositions of the two alloys are given in Table 1. The as-received materials were twin-belt continuous cast hot bands, which was produced using standard industrial practices. The thickness of AA 5754 and high-Fe AA 5754 hot bands were 2.82 and 3.28 mm, respectively. The hot bands possessed a typical deformed structure and a strong β fiber rolling texture. In order to generate a fully recrystallized structure prior to cold rolling, the hot bands of AA 5754 and high-Fe AA 5754 aluminum alloys were annealed at 399 °C for 3 h and 482 °C for 3 h, respectively, followed by air cooling. The grain structure of the annealed hot bands is shown in Fig. 1. It is seen that the recrystallized grains in the alloys were elongated along the RD. In order to investigate the effect of grain shape on texture evolution, the annealed hot bands were cold rolled to different reductions along the original RD and TD, respectively, on a laboratory rolling mill with rolls of 103 mm in diameter.

Texture measurements were performed at the quarter thickness of the cold rolled sheets. The (1 1 1), (2 0 0), and (2 2 0) pole figures were measured up to a maximum tilt angle of 75° by the Schulz back-reflection method using CuK_α radiation. The orientation distribution functions (ODFs) were calculated from the incomplete pole figures using the series expansion method ($l_{max} = 16$) [35]. The ODFs were presented as plots of constant φ_2 sections with isointensity contours in Euler space defined by the Euler angles φ_1, Φ and φ_2. The volume fractions of the texture components were calculated by an improved integration method [26,27].

Table 1
Chemical compositions of AA 5754 and high-Fe AA 5754 aluminum alloys (wt.%).

Alloy	Si	Fe	Cu	Mn	Mg	Cr	Al
5754	0.10	0.24	0.03	0.32	2.85	0.01	Bal.
High-Fe 5754	0.26	0.45	0.17	0.79	2.39	0.05	Bal.

3. Results

3.1. Texture evolution during rolling

The texture evolution of AA 5754 aluminum alloy during rolling along the original RD and TD is shown in Fig. 2(a) and (b), respectively. After annealing at 399 °C for 3 h, the recrystallization texture of AA 5754 aluminum alloy was characterized by the cube orientation with some scattering about the RD towards

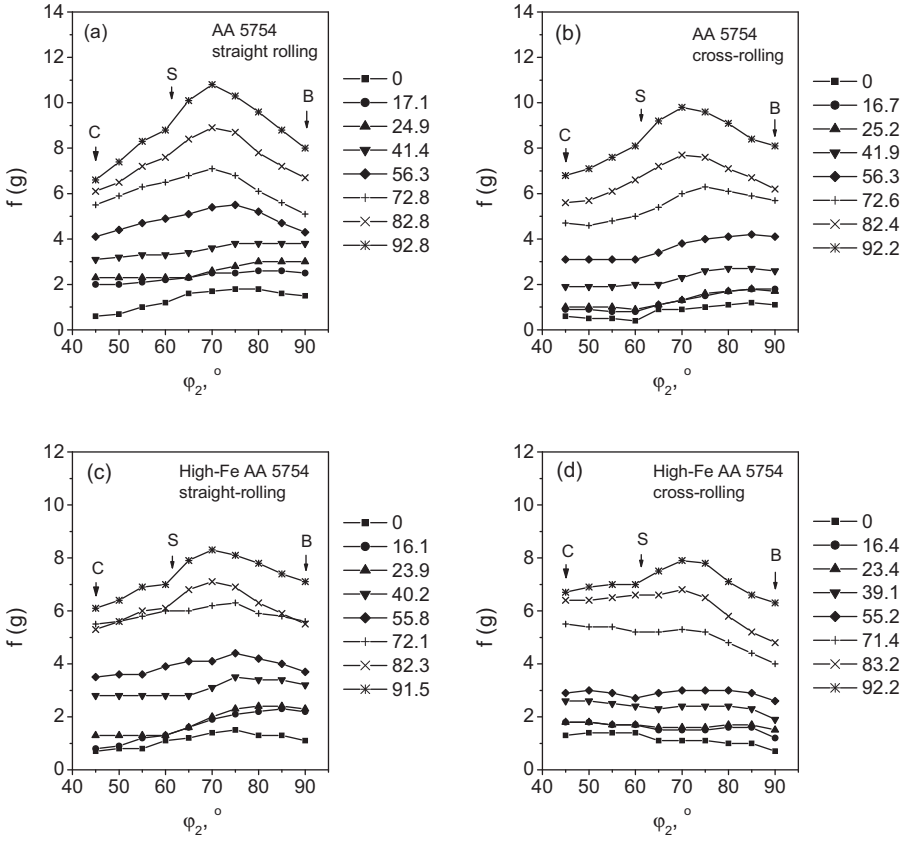

Fig. 4. Intensities of the ODF $f(g)$ at the center position of the β fiber as a function of a particular angle φ_2 in straight-rolled and cross-rolled AA 5754 and high-Fe AA 5754 aluminum alloys.

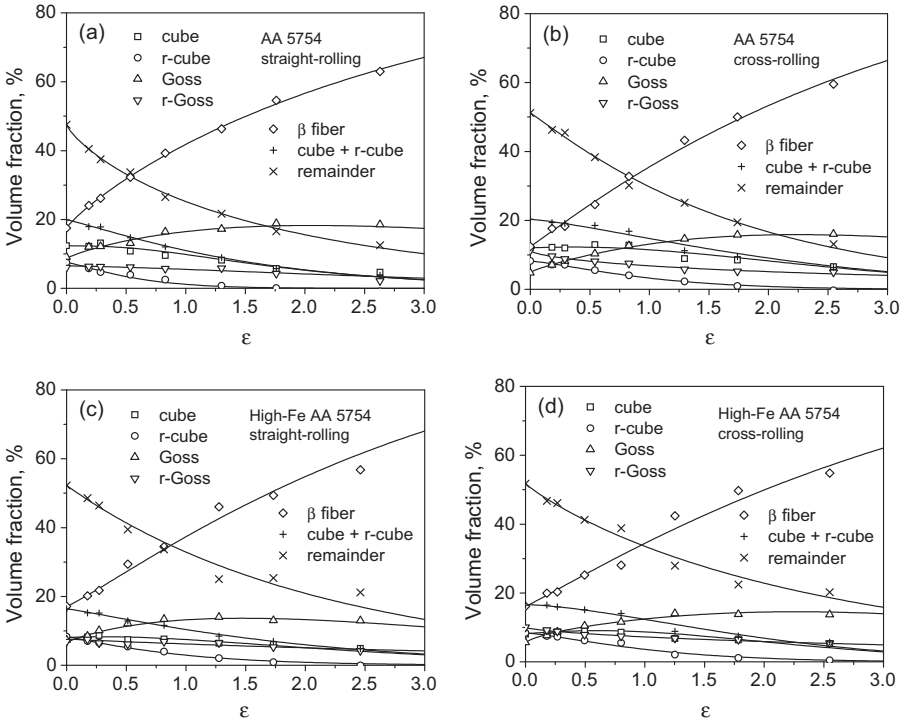

Fig. 5. Plots of texture volume fractions as a function of true rolling strain for straight-rolled and cross-rolled AA 5754 and high-Fe AA 5754 aluminum alloys. Points with different symbols are measured values, and sold lines are simulated results.

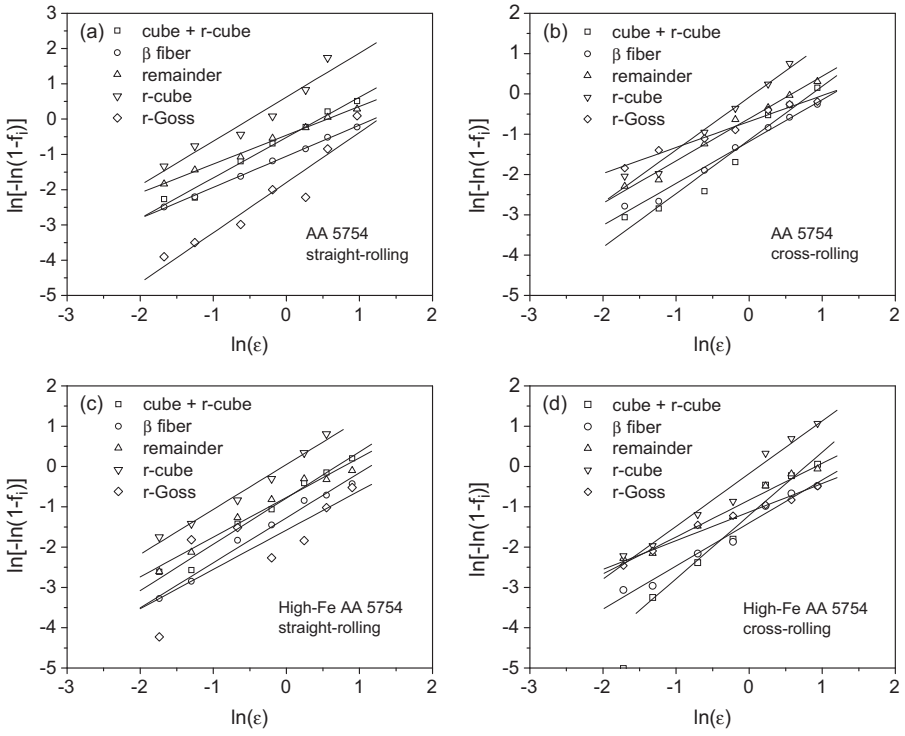

Fig. 6. $\ln[-\ln(1-f_i)]$ *vs.* $\ln\varepsilon$ for straight-rolled and cross-rolled AA 5754 and high-Fe AA 5754 aluminum alloys.

the Goss orientation. After 90° rotation about the normal direction (ND), the Goss orientation was transformed into the r-Goss $\{0\,1\,1\}\ \langle 0\,1\,1\rangle$ orientation. Thus, the initial texture was somewhat different during rolling along the original RD and TD. Initial orientations were gradually rotated to the β fiber during rolling. As the cold rolling reduction increased, the intensity of the cube orientation decreased, whereas the strength of the β fiber rolling texture increased. After 92% rolling reduction, a strong β fiber rolling texture was observed. The grain shape and slightly different initial textures, which were caused by 90° rotation about the ND, affected the texture evolution during rolling. It is noted that at a given reduction the strength of the β fiber rolling texture was slightly weaker in cross-rolling than in straight-rolling.

Fig. 3 shows the texture evolution of high-Fe AA 5754 aluminum alloy during rolling along the original RD and TD. After annealing at 482 °C for 3 h, the high-Fe AA 5754 aluminum alloy exhibited a very weak recrystallization texture, which was close to a random state. Thus, the initial texture was almost the same during rolling along the original RD and TD. The difference in texture evolution between straight-rolling and cross-rolling can be attributed to the effect of grain shape. Straight-rolling resulted in a slightly stronger β fiber rolling texture than cross-rolling.

A very condensed and comprehensive method for presenting the β fiber rolling texture is given in Fig. 4, where the intensities of orientations along the centerline of the β fiber are plotted as a function of the angle φ_2. It is noted that the overall

Table 2
Values of k_i and n_i in Eq. (2) for AA 5754 and high-Fe AA 5754 aluminum alloys.

Alloy	Rolling direction	Texture component	M_{i0} (%)	k_i	n_i	r
5754	RD	Cube + r-cube	19.9	0.59 (0.56–0.63)	1.14 ± 0.06	0.992
		β Fiber	17.5	0.35 (0.34–0.35)	0.88 ± 0.02	0.999
		Remainder	47.5	0.63 (0.62–0.65)	0.82 ± 0.03	0.997
		r-Cube	7.5	1.87 (1.60–2.17)	1.25 ± 0.16	0.967
		r-Goss	6.5	0.16 (0.14–0.20)	1.42 ± 0.20	0.954
	TD	Cube + r-cube	20.3	0.32 (0.28–0.36)	1.33 ± 0.14	0.975
		β Fiber	12.4	0.31 (0.29–0.32)	1.04 ± 0.06	0.993
		Remainder	51.2	0.54 (0.51–0.57)	1.05 ± 0.06	0.992
		r-Cube	8.2	0.92 (0.83–1.02)	1.31 ± 0.11	0.987
		r-Goss	11.3	0.50 (0.48–0.52)	0.64 ± 0.04	0.989
High-Fe 5754	RD	Cube + r-cube	16.4	0.46 (0.43–0.49)	1.15 ± 0.07	0.991
		β Fiber	17.1	0.28 (0.26–0.30)	1.12 ± 0.06	0.992
		Remainder	52.3	0.46 (0.43–0.50)	0.98 ± 0.08	0.984
		r-Cube	8.4	1.05 (0.98–1.12)	1.11 ± 0.07	0.992
		r-Goss	7.6	0.21 (0.15–0.28)	0.97 ± 0.32	0.802
	TD	Cube + r-cube	16.6	0.30 (0.27–0.33)	1.57 ± 0.14	0.985
		β Fiber	16.1	0.25 (0.23–0.26)	1.07 ± 0.07	0.988
		Remainder	51.8	0.43 (0.41–0.46)	0.91 ± 0.06	0.988
		r-Cube	8.4	0.84 (0.76–0.92)	1.31 ± 0.10	0.986
		r-Goss	10.0	0.32 (0.31–0.34)	0.71 ± 0.05	0.990

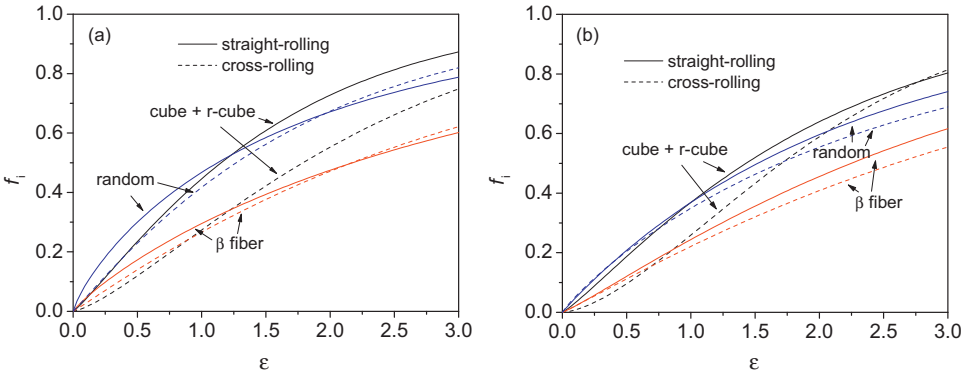

Fig. 7. Comparison of the texture evolution between straight-rolling and cross-rolling for (a) AA 5754 and (b) high-Fe AA 5754 aluminum alloys.

texture sharpness increased with increasing rolling reduction for AA 5754 and high-Fe AA 5754 aluminum alloys. At large reductions, the maximum intensity of the β fiber was located at $\varphi_2 = 70^\circ$, which became a dominant rolling texture component. The grain shape had no significant effect on the distribution of orientation intensities along the β fiber.

3.2. Quantitative analysis of texture evolution

The texture evolution during rolling can be analyzed quantitatively in terms of the variation in the texture volume fractions with rolling reduction. The volume fractions of the cube, r-cube, Goss, r-Goss, β fiber and remainder components, which were calculated by an improved integration method [26,27], are plotted in Fig. 5 as a function of true rolling strain. As the true rolling strain increased, the volume fractions of the cube, r-cube, r-Goss and remainder components decreased, whereas the volume fraction of the β fiber component increased. The volume fraction of the Goss component increased with increasing true rolling strain. When the true rolling strain reached the range of 1.2–2.5, the volume fraction of the Goss component changed slightly.

In order to quantify the texture evolution during rolling, we have established an empirical relationship between the texture volume fractions and true rolling strain [26,27]. The variation in the texture volume fractions with true rolling strain is defined by:

$$f_i = \frac{M_i - M_{i0}}{M_{i\infty} - M_{i0}} \quad (1)$$

where M_{i0}, M_i and $M_{i\infty}$ are the texture volume fractions prior to deformation, at true rolling strain and at the end of the texture forming process, respectively. For the cube + r-cube, remainder, r-cube, and r-Goss components, the $M_{i\infty}$ value is 0, while it is 1 for the β fiber component. The relationship between the value of f_i and true rolling strain (ε) can be described by the JMAK equation:

$$f_i = 1 - \exp(-k_i \varepsilon^{n_i}) \quad (2)$$

where k_i is an empirical constant, and n_i is the strain exponent for the texture components. The data for the f_i can be presented in the form of a $\ln[-\ln(1-f_i)]$ *vs.* $\ln\varepsilon$, as shown in Fig. 6. The values of k_i and n_i were determined by fitting the experimental data using Eq. (2). Table 2 shows the values of k_i and n_i as well as the correlation coefficient (r) of the linear fits. Fig. 5 shows the comparison of the calculated and measured texture volume fractions for AA 5754 and high-Fe AA 5754 aluminum alloys. It is seen that the texture evolution during rolling was better simulated by the JMAK equation. Thus, the effect of grain shape on texture evolution can be more accurately determined by the values of k_i and n_i than direct comparison of ODFs.

4. Discussion

During rolling initial orientations are gradually rotated into the β fiber component. As the true rolling strain increases, the volume fractions of the cube, r-cube, r-Goss and remainder components decrease, whereas the volume fraction of the β fiber component increases. The texture evolution during rolling can be quantified in terms of a simple relation between the texture volume fractions and true rolling strain. Thus, the effect of initial microstructure and texture on rolling texture evolution can be quantitatively revealed by the values of k_i and n_i. It is seen from Table 2 that the k_i value for the cube + r-cube component is significantly larger in straight-rolling than in cross-rolling, while it is slightly larger for the β fiber and remainder components. In order to clearly reveal the difference in the development of different texture components, the f_i value in straight-rolled and cross-rolled sheets was calculated based on the values of k_i and n_i, as shown in Fig. 7. It is obvious that the k_i value in Eq. (2) reflects the rate of formation or disappearance of each texture component. Straight-rolling results in a higher rate of disappearance of the r-cube + cube component and a slightly higher rate of formation of the β fiber component than cross-rolling.

The difference in texture evolution between straight-rolling and cross-rolling can be attributed to different initial microstructures and textures caused by changing the rolling direction. For the high-Fe AA 5754 aluminum alloy, the initial texture is almost the same in straight-rolling and cross-rolling (Fig. 3). It means that the difference in texture evolution comes from the effect of grain shape. The elongated grains in the RD are easier to rotate from initial orientations to the β fiber in straight-rolling than in cross-rolling. For the AA 5754 aluminum alloy, the initial texture is slightly different in straight-rolling and cross-rolling (Fig. 2). Since the cube + r-cube component has almost the same volume fraction, the higher rate of disappearance of the r-cube + cube component in straight-rolling can be attributed to the effect of grain shape.

Crystal lattice rotation during deformation depends on the potential active slip systems. Grains with different orientations have different slip patterns, leading to different lattice rotations. Thus, each individual texture component has its own lattice rotation kinetics different from the other texture components. The quantitative analysis of texture volume fractions may give more information on the evolution of different texture components. Fig. 7 shows that the grain shape has a more significant effect on the evolution of the cube + r-cube component than that of the other components.

5. Conclusions

AA 5754 and high-Fe AA 5754 aluminum alloys with elongated grains were cold rolled to different reductions along the original

RD and TD, respectively. The effect of grain shape on the texture evolution during rolling was investigated by X-ray diffraction. The following conclusions are drawn from this study.

(1) The hot bands of AA 5754 and high-Fe AA 5754 aluminum alloys possess a typical deformed structure and a strong β fiber rolling texture. After recrystallization annealing, the elongated grains in the RD are observed. The recrystallization texture of AA 5754 aluminum alloy is characterized by the cube orientation with some scattering about the RD towards the Goss orientation, while the recrystallization texture of high-Fe AA 5754 aluminum alloy is close to a random state.
(2) The grain shape and slightly different initial textures, which are caused by 90° rotation about the ND, affect the texture evolution during rolling. At a given reduction the strength of the β fiber rolling texture is slightly weaker in cross-rolling than in straight-rolling.
(3) The texture evolution of AA 5754 and high-Fe AA 5754 aluminum alloys with elongated grains during rolling along the original RD and TD was quantified in terms of a simple relation between the texture volume fractions and true rolling strain. The k_i value in the relation reflects the rate of formation or disappearance of each texture component. Straight-rolling results in a higher rate of disappearance of the r-cube + cube component and a slightly higher rate of formation of the β fiber component than cross-rolling.
(4) For the high-Fe AA 5754 aluminum alloy, the difference in texture evolution between straight-rolling and cross-rolling can be attributed to the effect of grain shape. The elongated grains in the RD are easier to rotate from initial orientations to the β fiber in straight-rolling than in cross-rolling.

Acknowledgment

This work was supported by the National Natural Science Foundation of China (grant no. 50874097).

References

[1] J. Hirsch, K. Lücke, Acta Metall. 36 (1988) 2863–2882.
[2] O. Engler, J. Hirsch, K. Lücke, Acta Metall. 37 (1989) 2743–2753.
[3] R.K. Roy, S. Kar, S. Das, J. Alloys Compd. 468 (2009) 122–129.
[4] J. Sarkar, S. Saimoto, B. Mathew, P.S. Gilman, J. Alloys Compd. 479 (2009) 719–725.
[5] Y.L. Deng, L. Wan, Y. Zhang, X.M. Zhang, J. Alloys Compd. 498 (2010) 88–94.
[6] W.B. Hutchinson, A. Oscarsson, A. Karlsson, Mater. Sci. Technol. 5 (1989) 1118–1127.
[7] A. Oscarsson, W.B. Hutchinson, H.E. Ekstrom, Mater. Sci. Technol. 7 (1991) 554–564.
[8] W.C. Liu, T. Zhai, C.-S. Man, B. Radhakrishnan, J.G. Morris, Philos. Mag. 84 (2004) 3305–3321.
[9] X.Y. Kong, W.C. Liu, J. Li, H. Yuan, J. Alloys Compd. 491 (2010) 301–307.
[10] N. Hansen, D. Juul Jensen, Metall. Trans. A 17 (1986) 253–259.
[11] O. Engler, Textures Microstruct. 23 (1995) 61–86.
[12] A. Duckham, R.D. Knutsen, O. Engler, Acta Mater. 49 (2001) 2739–2749.
[13] R. Jayaganthan, H.-G. Brokmeier, B. Schwebke, S.K. Panigrahi, J. Alloys Compd. 496 (2010) 183–188.
[14] P. Van Houtte, Mater. Sci. Eng. 55 (1982) 69–77.
[15] J. Hirsch, K. Lücke, Acta Metall. 36 (1988) 2883–2904.
[16] L. Delannay, S.R. Kalidindi, P. Van Houtte, Mater. Sci. Eng. A 336 (2002) 233–244.
[17] L.S. Tóth, K.W. Neale, J.J. Jonas, Acta Metall. 37 (1989) 2197–2210.
[18] Y. Zhou, K.W. Neale, L.S. Tóth, Acta Metall. Mater. 40 (1992) 3179–3193.
[19] G.B Sarma, B. Radhakrishnan, T. Zacharia, Comput. Mater. Sci 12 (1998) 105–123.
[20] P. Van Houtte, L. Delannay, S.R. Kalidindi, Int. J. Plast. 18 (2002) 359–377.
[21] O. Engler, M. Crumbach, S. Li, Acta Mater. 53 (2005) 2241–2257.
[22] B. Holmedal, P. Van Houtte, Y. An, Int. J. Plast. 24 (2008) 1360–1379.
[23] R. Sebald, G. Gottstein, Acta Mater. 50 (2002) 1587–1598.
[24] M. Crumbach, M. Goerdeler, G. Gottstein, Acta Mater. 54 (2006) 3275–3289.
[25] M. Crumbach, M. Goerdeler, G. Gottstein, Acta Mater. 54 (2006) 3291–3306.
[26] W.C. Liu, J.G. Morris, Mater. Sci. Eng. A 339 (2003) 183–193.
[27] W.C. Liu, J.G. Morris, Metall. Trans. A 35 (2004) 265–277.
[28] W.C. Liu, Z. Li, C.-S. Man, D. Raabe, J.G. Morris, Mater. Sci. Eng. A 434 (2006) 105–113.
[29] Q. Zeng, X. Wen, T. Zhai, Mater. Sci. Eng. A 476 (2008) 290–300.
[30] W.C. Liu, X.Y. Kong, M.B. Chen, J. Li, H. Yuan, Q.X. Yang, Mater. Sci. Eng. A 516 (2009) 263–269.
[31] W.C. Liu, C.-S. Man, D. Raabe, Mater. Sci. Eng. A 537 (2010) 1249–1254.
[32] K.K. Cho, Y.H. Chung, C.W. Lee, S.I. Kwun, M.C. Shin, Scripta Mater. 40 (1999) 651–657.
[33] Y.H. Chung, K.K. Cho, J.H. Han, M.C. Shin, Scripta Mater. 43 (2000) 759–764.
[34] L. Delannay, M.A. Melchior, J.W. Signorelli, J.-F. Remacle, T. Kuwabara, Comput. Mater. Sci. 45 (2009) 739–743.
[35] H.J. Bunge, Texture Analysis in Materials Science, Butterworths, London, 1982.